Article



# Lipid Nanoparticle-Encapsulated Polyl:C as an Adjuvant Enhances Both Humoral and Cellular Immune Responses to the Hepatitis B Vaccine

Zhixian Zhao , Bin Wang , Hao Wang , Qiang Zhang , Yunfei Liang , Yuan Liu *

Posted Date: 2 April 2026

doi: 10.20944/preprints202604.0040.v1

Keywords: lipid nanoparticle; polyinosinic-polycytidylic acid; HBsAg; adjuvant; immunogenicity

 doi:10.20944/preprints202604.0040.v1



*Article*

# Lipid Nanoparticle-Encapsulated PolyI:C as an Adjuvant Enhances Both Humoral and Cellular Immune Responses to the Hepatitis B Vaccine

**Zhixian Zhao [1], Bin Wang [2], Hao Wang [1], Qiang Zhang [2], Yunfei Liang [2] and Yuan Liu [1,*]**

[1] Lake Shore Biotechnology (Beijing) Co., Ltd., Beijing 100176, China

[2] Liaoning Yisheng Biopharmaceutical Co., Ltd., Shenyang 110136, China

* Correspondence: purpletea@hotmail.com

**Abstract**

**Background**: Currently marketed hepatitis B vaccines are primarily recombinant protein vaccines. However, their antigen immunogenicity is relatively weak, requiring combination with effective adjuvants to enhance the immune response. The development of novel, highly effective adjuvants is a key strategy for optimizing vaccine performance. Polyinosinic-polycytidylic acid (PolyI:C), a synthetic double-stranded RNA analog, activates TLR3/RLR pathways to enhance T-cell priming and cellular immunity. However, its utility as a sole adjuvant is limited by rapid nuclease degradation and poor cytosolic delivery. Lipid nanoparticles (LNPs), a mature delivery platform, enable high encapsulation efficiency, efficient cellular uptake, and endosomal escape. **Objectives**: This study aimed to evaluate the adjuvant effect of LNP-encapsulated PolyI:C (LNP-PolyI:C) on the immunogenicity of hepatitis B surface antigen (HBsAg) in vivo. **Methods**: The colloidal stability of LNP-PolyI:C stored at 2–8 °C for 9 months was monitored using dynamic light scattering (DLS) on a Zetasizer Lab instrument. Serum levels of HBsAg-specific IgG, IgG1, and IgG2a antibodies in immunized Kunming mice were measured by enzyme-linked immunosorbent assay (ELISA). The secretion of HBsAg-specific cytokines by splenocytes was analyzed using flow cytometry and enzyme-linked immunospot (ELISpot) assay. **Results**: The results demonstrated that the LNP-encapsulated PolyI:C adjuvant significantly increased the secretion of HBsAg-specific IFN-γ, IL-2, and TNF-α by murine splenocytes, indicating a Th1-biased and cytotoxic T lymphocyte (CTL)-mediated cellular immune response. In addition, this formulation markedly elevated serum titers of HBsAg-specific IgG, IgG1, and IgG2a. Notably, the increased IgG2a/IgG1 ratio highlights a robust enhancement of the humoral immune response. **Conclusions**: These findings underscore the advantages of the LNP-PolyI:C adjuvant in enhancing both humoral and cellular immunity, demonstrating its considerable potential as a novel adjuvant.

**Keywords:** lipid nanoparticle; polyinosinic-polycytidylic acid; HBsAg; adjuvant; immunogenicity

## 1. Introduction

Vaccination is one of the most effective methods for controlling infectious diseases and a widely used intervention in public health practice[1]. Hepatitis B is an infectious disease caused by the hepatitis B virus (HBV). Long-term HBV infection can cause varying degrees of liver damage and may progressively develop into hepatitis, liver fibrosis, cirrhosis, and hepatocellular carcinoma[2]. Hepatitis B vaccination can effectively prevent hepatitis B, limit the progression of symptoms in carriers, and reduce the disease burden [3].

Recombinant protein and peptide subunit antigens typically exhibit weak immunogenicity and are often insufficient to induce robust protective humoral and cellular immune responses[4,5]. Consequently, most subunit antigens require co-formulation with adjuvants. Adjuvants are immunomodulatory substances added to vaccines that play a crucial role in regulating the host

 doi:10.20944/preprints202604.0040.v1



immune response, such as enhancing immunogenicity and reducing the required antigen dose[4,6]. Currently, the majority of licensed hepatitis B vaccines rely on aluminium-based adjuvants. Prominent examples include Recombivax HB (Merck & Co., USA), Engerix-B (GlaxoSmithKline Biologicals, USA), and several recombinant vaccines produced in China, such as those expressed in Saccharomyces cerevisiae (China National Biotec Group), *Hansenula polymorpha* (AIM Vaccine Co., Ltd.), and CHO cells (North China Pharmaceutical Company Ltd.)[6–8]. Aluminium adjuvants function through multiple mechanisms. They adsorb antigens via electrostatic interactions, creating a depot effect that slows antigen release and promotes the recruitment and accumulation of antigen-presenting cells (APCs) at the injection site. This process facilitates antigen uptake, processing, and presentation. In addition, aluminium adjuvant can activate dendritic cells. Following phagocytosis, it activates the NLRP3 inflammasome, leading to the release of active IL-1β and IL-18[9]. Studies have shown that aluminium adjuvants can induce a Th2-biased immune response but are weak inducers of Th1 immune responses[9,10]. Therefore, aluminium adjuvants are suboptimal for viral diseases that rely on Th1-mediated immunity and the priming of cytotoxic CTLs. In addition, the recombinant hepatitis B vaccine Heplisav B, developed by Dynavax Technologies Corporation (USA), contains the CpG 1018 adjuvant. CpG 1018 is a negatively charged 22-base oligonucleotide that activates Toll-like receptor 9 (TLR9) and induces a Th1 immune response[4]. However, studies have reported that compared to adults receiving the Engerix-B, those receiving the Heplisav B exhibited higher reported rates of acute myocardial infarction, herpes zoster, and death[11]. These limitations underscore the need for novel adjuvant systems that can safely and effectively elicit both robust humoral and Th1-biased cellular immunity.

PolyI:C is a synthetic analog of double-stranded RNA (dsRNA) that functions as a pathogen-associated molecular pattern (PAMP) and activates multiple innate immune receptors located in endosomal and cytoplasmic compartments[12]. In antigen-presenting cells, endosomal PolyI:C is sensed by TLR3, whereas cytoplasmic PolyI:C engages RLRs, including RIG-I and melanoma differentiation–associated protein 5 (MDA-5)[13]. TLR3 signaling proceeds through the TIR-domain–containing adaptor-inducing interferon-β (TRIF), leading to activation of interferon regulatory factor 3 (IRF3), nuclear factor κB (NF-κB), and activator protein-1 (AP-1), which collectively drive the production of type I interferons and pro-inflammatory cytokines[14,15]. In contrast, RLR engagement triggers receptor oligomerization, exposure of the N-terminal caspase recruitment domain (CARD), and mitochondrial translocation. Subsequent signaling through the mitochondrial antiviral signaling (MAVS) protein robustly induces type I and III interferons, which promote type 1 cytokine responses[13]. The resulting type I interferon milieu enhances natural killer cell activity, supports antigen-specific $CD8^+$ T cell responses, and promotes dendritic cell maturation, thereby linking innate immune sensing of PolyI:C to the development of effective antiviral and adaptive immune responses[16]. However, when administered alone as a vaccine adjuvant, PolyI:C is rapidly degraded by ubiquitous nucleases and reaches the cytosol inefficiently[17]. This short half-life and poor intracellular access blunt its immunopotentiating activity, while also requiring higher doses that can trigger systemic hyperinflammation. These higher doses increase the risk of excessive immune activation and autoimmunity [18,19]. Therefore, to address these issues and enhance the stability and safety of PolyI:C, researchers have developed various delivery platforms, including polymer films[20], hydrogels[21,22], and various micro and nanoparticle systems[23,24]. Among these, LNPs have emerged as a particularly promising candidate due to their efficient encapsulation and cytosolic delivery capabilities[25,26].

LNPs are nanoparticles composed of ionizable cationic lipids, other lipid types, and encapsulated cargo, and they are recognized as the most mature delivery platform. The success of LNP-containing mRNA vaccines, such as Comirnaty and Spikevax, during the COVID-19 pandemic has underscored the immense potential of LNP technology[27,28]. All currently FDA-approved LNP formulations employ a four-component lipid composition: an ionizable cationic lipid, a neutral helper lipid, cholesterol, and a PEG-lipid conjugate[29,30]. The intracellular delivery efficiency of LNPs relies on the protonation of the ionizable cationic lipid in the acidic endosomal environment; this

 doi:10.20944/preprints202604.0040.v1



process disrupts endosomal membrane integrity, facilitating the release of the encapsulated cargo. Helper phospholipids provide structural support during LNP formation and may participate in endosomal escape processes associated with membrane fusion. Cholesterol modulates membrane rigidity and integrity, contributing to particle structural stability while regulating in vivo delivery efficiency and organ distribution tendencies. Surface PEGylation inhibits protein adsorption and particle aggregation through steric hindrance, thereby prolonging circulation time and ensuring uniform particle size [30–32]. Based on the aforementioned structural and functional characteristics of LNPs, encapsulating PolyI:C within lipid nanoparticle systems can effectively protect it from nuclease degradation, thereby fully unleashing its potential as a vaccine adjuvant.

Herein, we demonstrate that LNP encapsulation significantly potentiates the innate immunostimulatory activity of PolyI:C compared to either soluble PolyI:C or empty LNPs alone. Mechanistically, whereas sole engagement of TLR3 yielded suboptimal adjuvant efficacy, the concomitant activation of TLR3 and RLRs elicited robust adaptive immune responses. In vivo, intramuscular co-administration of recombinant HBsAg with LNP-encapsulated PolyI:C in mice elicited antigen-specific antibody titers surpassing those induced by soluble PolyI:C, while concurrently augmenting cellular immune responses.

## 2. Materials and Methods

### *2.1. LNP Encapsulating PolyI:C and Vaccine Preparation*

The HBsAg and PolyI:C used in this study were both prepared in-house. HBsAg was expressed in Pichia pastoris and subsequently purified. PolyI:C was formed by annealing high-molecular-weight polyinosinic acid and polycytidylic acid under specific salt concentration conditions, followed by sterile filtration and aliquoting for storage. LNP-PolyI:C was synthesized by CATUG Biotechnology (Suzhou) Co., Ltd. Briefly, the lipid components (DOTAP/DSPC/Cholesterol/DSPE-PEG2000) were dissolved in ethanol at a specific molar ratio. Subsequently, the lipid mixture was combined with a phosphate-buffered saline (PBS) solution containing PolyI:C at a defined volume ratio using a microfluidic mixer (Micro & Nano). In parallel, empty LNP without PolyI:C were prepared as a control. The resulting LNP-PolyI:C formulations were characterized for their Z-average size and polydispersity index (PDI) using a Zetasizer Lab instrument (Malvern Panalytical, UK). Their colloidal stability was then assessed by monitoring these parameters over time during storage at 2–8 °C. The compositions of the designed vaccines are shown in Table 1.

**Table 1.** The compositions of the vaccines.

| Vaccine Group | Vaccine Ingredients (per milliliter) | | | |
|---|---|---|---|---|
| | HBsAg (μg) | LNP-PolyI:C (μg) | PolyI:C (μg) | Empty LNP |
| LNP-PolyI:C+HBsAg | 40 | 1000 | | |
| PolyI:C+HBsAg | 40 | | 1000 | |
| Empty LNP+HBsAg | 40 | | | The volume of the empty LNP is the same as that of LNP-PolyI:C. |
| HBsAg | 40 | | | |
| PBS | | | | |

### *2.2. Animal Experiments*

Female Kunming mice (13-16 g), specific pathogen-free (SPF), were purchased from Liaoning Changsheng Biotechnology Co., Ltd. (Benxi, China). Upon arrival at the institutional animal facility, the mice were housed in a barrier environment (temperature: 20 °C–25 °C; humidity: 40%–70%; 12

 doi:10.20944/preprints202604.0040.v1



h:12 h light-dark cycle) and fed a standard maintenance diet. After an acclimatization period of 3–5 days, the mice were randomly assigned to 5 groups (N = 8 per group) before immunization. According to the vaccine groups outlined in Table 1, each mouse was administered 100 μL of vaccine via intramuscular (i.m.) injection on days 0 and 14. Blood samples were collected from the retro-orbital venous plexus on days 14 and 28, and serum was separated for ELISA. On day 28, the mice were euthanized, and spleens were harvested for subsequent flow cytometry and ELISpot analysis.

*2.3. Enzyme-Linked Immunosorbent Assay*

The titers of HBsAg-specific total IgG, IgG1, and IgG2a antibodies in immune sera were determined using ELISA. The procedure was briefly described as follows: First, ELISA plates were coated with HBsAg (2 μg/mL, 100 μL/well) and incubated overnight at 4 °C. The plates were then blocked with PBS containing 3% bovine serum albumin (3% BSA-PBS) at 37 °C for 1 hour. Subsequently, serially diluted serum samples (diluted in 1.5% BSA-PBS) were added to the plates and incubated at room temperature for 1 hour, followed by the addition of horseradish peroxidase (HRP)-conjugated secondary antibodies diluted in 1.5% BSA-PBS. The secondary antibodies included goat anti-mouse IgG(H+L) (Gene-Protein Link, Cat# P03S01, China), IgG1 (SouthernBiotech, Cat# 1070-05, USA), and IgG2a (SouthernBiotech, Cat# 1080-05, USA), which were incubated at 37 °C for 1 hour. Finally, 100 μL of tetramethylbenzidine (TMB) substrate solution (Solarbio, Cat# PR1200, China) was added to each well, and the mixture was incubated at 37 °C for 10 minutes. The reaction was terminated by adding 50 μL of 2 M sulfuric acid. After each step, the plates were washed three times with PBS containing 0.05% Tween-20. Absorbance was measured immediately at 450 nm and 630 nm using a Synergy H1 microplate reader (BioTek, USA), with blank wells used for zero adjustment. A sample was considered positive if its OD450 value was at least 2.1 times that of the negative control.

*2.4. Isolation of Splenocytes*

Under a sterile laminar flow hood, the spleen was placed in a 70 μm cell strainer (BD, USA) positioned over a 50 mL centrifuge tube. The spleen was gently ground, and splenocytes were flushed out with 10 mL of PBS. Following centrifugation, the supernatant was discarded, and the cell pellet was resuspended in 5 mL of 1×red blood cell (RBC) lysis buffer (BioLegend, Cat# 420301, USA), followed by incubation at 4 °C for 3 minutes. The reaction was terminated by adding 15 mL of PBS. After subsequent centrifugation, the supernatant was discarded, and the cells were washed once with 10 mL of RPMI 1640 medium (Gibco, Cat# 11875-093, USA). Finally, the cells were resuspended in RPMI 1640 medium supplemented with 10% fetal bovine serum (Gibco, Cat# 10099-141C, USA) and 1% penicillin–streptomycin (Solarbio, Cat# P7630, China). After cell counting, the cell suspension was diluted to $5 \times 10^6$ cells/mL.

*2.5. Flow Cytometry Analysis*

Multicolor flow cytometry was employed to assess cytokine secretion in splenocytes. Briefly, 800 μL of cell suspension was added to a 24-well plate and co-cultured overnight with the HBsAg peptide pool at 37 °C and 5% $CO_2$. Subsequently, Brefeldin A Solution (Biolegend, Cat# 420601, USA) was added, and incubation continued for an additional 4 hours under the same conditions to block cytokine release. Following incubation, cells were washed with PBS. Dead cells were labeled using the Zombie NIR Fixable Viability Kit (Biolegend, Cat# 423105, USA), and Fc receptors were blocked using TruStain FcX PLUS (anti-mouse CD16/32) (Biolegend, Cat# 156603, USA). Both steps were performed at room temperature in the dark. The cells were then incubated for 30 minutes at 4 °C in the dark with the following fluorescently conjugated antibodies: FITC-labeled anti-CD3, PerCP-Cy5.5-labeled anti-CD4, and AF700-labeled anti-CD8a. After fixation and permeabilization, cells were incubated for 30 minutes at room temperature in the dark with the following intracellular cytokine antibodies: PE-Cy7-labeled anti-TNF-α, APC-labeled anti-IFN-γ, PE-labeled anti-IL-6,

 doi:10.20944/preprints202604.0040.v1



BV605-labeled anti-IL-4, and BV421-labeled anti-IL-2. Following washes with permeabilization wash buffer and PBS, cells were analyzed using a BD FACSCelesta flow cytometer (BD, USA). Data analysis was performed using FlowJo software (BD, USA).

### *2.6. Enzyme-Linked Immunospot Assay*

A FluoroSpot assay was performed using the FluoroSpot Plus: Mouse IFN-γ/IL-4 kit (MabTech, Cat# FSP-3146-10, Sweden) according to the manufacturer's protocol. Briefly, 96-well plates were washed with sterile PBS and blocked with cell culture medium. Following this, 100 μL of cell suspension was added to each well. The wells were then stimulated with 100 μL of HBsAg peptide pool (test samples), phytohemagglutinin (DAKEWE, Cat# 2030411, China) (positive control), or cell culture medium (negative control). All conditions were set up in triplicate. The plates were incubated in a cell culture incubator at 37 °C with 5% $CO_2$ for 24 hours. After incubation, the cell culture supernatant was discarded, and the plates were processed according to the kit protocol, which involved sequential incubation with detection monoclonal antibodies, fluorophore-conjugated secondary antibodies, and FluoroSpot enhancer solution. Finally, the plates were left to dry overnight at room temperature in the dark. The number of fluorescent spots in each well was detected using the Mabtech IRIS™ 2 instrument (MabTech, Sweden), and the resulting data were exported for analysis. The mean number of spots ± SEM in triplicate wells was calculated and expressed as spots forming cells (SFCs) per $10^6$ splenocytes.

### *2.7. Statistical Analysis*

All data in this study are expressed as mean ± SEM. Statistical analyses were performed using GraphPad Prism 9 software (GraphPad Software Inc., La Jolla, CA, USA). Multiple comparisons were performed using one-way analysis of variance (ANOVA) followed by Tukey's honestly significant difference (HSD) test. $P < 0.05$ was considered statistically significant (*$p < 0.05$；**$p < 0.01$；***$p < 0.001$；****$p < 0.0001$).

## 3. Results

### *3.1. Stability Results of LNP-PolyI:C*

Following the method reported by Singh et al.[33], PolyI:C was encapsulated into LNPs using the hydrodynamic focusing (HDF) technique. A lipid stream (containing DOTAP, DSPC, CHOL, and DSPE-PEG 2000) dissolved in ethanol and a PolyI:C solution dissolved in PBS were mixed at a specific volumetric flow ratio within a microfluidic chip (Figure 1A-B). The colloidal stability of LNP-PolyI:C stored at 2–8 °C for 9 months was monitored using DLS on a Zetasizer Lab instrument. As shown in Figure 1C, the Z-average size and PDI of LNP-PolyI:C exhibited dynamic changes characterized by an initial increase followed by stabilization. Both parameters peaked at the 2-month time point (123 nm and 0.41, respectively) and then plateaued.

 doi:10.20944/preprints202604.0040.v1



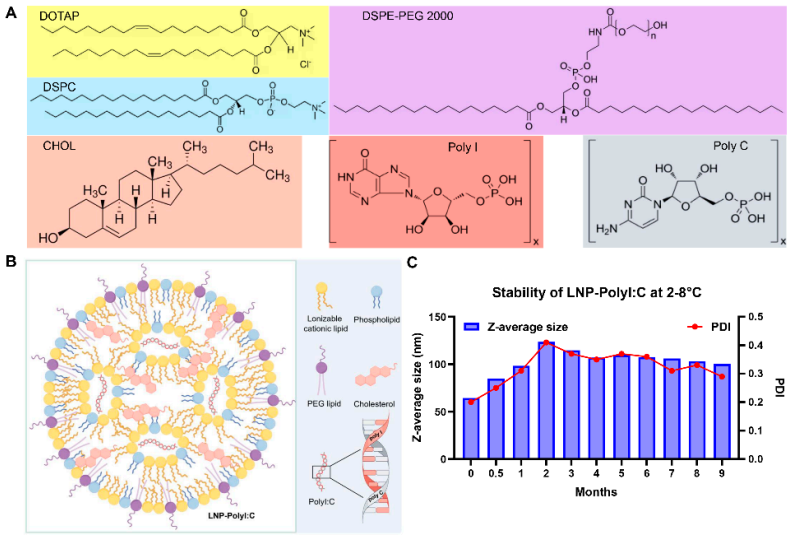


**Figure 1.** Composition and stability results of LNP-PolyI:C. (**A**) Chemical structures of the components constituting LNP-PolyI:C. (**B**) Schematic diagram of the LNP-PolyI:C structure. The figure was created with Figdraw (www.figdraw.com). (**C**) The colloidal stability of LNP-PolyI:C stored at 2–8 °C for 9 months. DOTAP: 1,2-stearoyl-3-trimethylammonium-propane, DSPC: 1,2-distearoyl-sn-glycero-3-phosphocholine, CHOL: cholesterol, DSPE-PEG 2000: 1,2-distearoyl-sn-glycero-3-phosphoethanolamine-N-[methoxy(polyethylene glycol)-2000].

### *3.2. The LNP-PolyI:C Adjuvant Significantly Enhances Serum Antibody Response Levels*

To evaluate the ability of the LNP-PolyI:C adjuvant to induce neutralizing antibodies, an immunogenicity study of the LNP-PolyI:C/HBsAg vaccine was conducted in mice. The experimental procedure is shown in Figure 2A. Animals were immunized according to a 0- and 14-day schedule, with each mouse receiving 4 μg of HBsAg by intramuscular injection at each dose. PBS injection served as the negative control. The study consisted of five groups: LNP-PolyI:C+HBsAg, PolyI:C+HBsAg, empty LNP+HBsAg, HBsAg alone, and PBS. Blood samples were collected from the retro-orbital venous plexus on day 14 (D14) and day 28 (D28) after the primary immunization. ELISA measured serum levels of HBsAg-specific total IgG, IgG1, and IgG2a antibodies. The results demonstrated that the LNP-PolyI:C adjuvant group induced a robust early humoral immune response as early as day 14 post-primary immunization. The IgG1 titer in this group was significantly higher than that in the other four groups ($P < 0.01$). The total IgG titer was significantly higher than that in the PolyI:C+HBsAg group, the HBsAg-alone group, and the PBS group ($P < 0.05$), but no statistically significant difference was observed compared to the empty LNP+HBsAg group ($P > 0.05$) (Figure 2B). Although the IgG2a titer did not differ significantly from that in the other four groups ($P > 0.05$), it was the highest among all groups (Figure 2F). On day 14 post-booster immunization (D28), all vaccinated groups, except the negative control, mounted a robust anamnestic response, with total IgG, IgG1, and IgG2a titers exceeding those observed after primary immunization. The levels of all three HBsAg-specific antibodies in the LNP-PolyI:C adjuvant group were significantly higher than those in the other four groups ($P < 0.05$), with only IgG1 showing no statistically significant difference compared to the Empty LNP + HBsAg group ($P > 0.05$) (Figure 2C, E, G).

 doi:10.20944/preprints202604.0040.v1



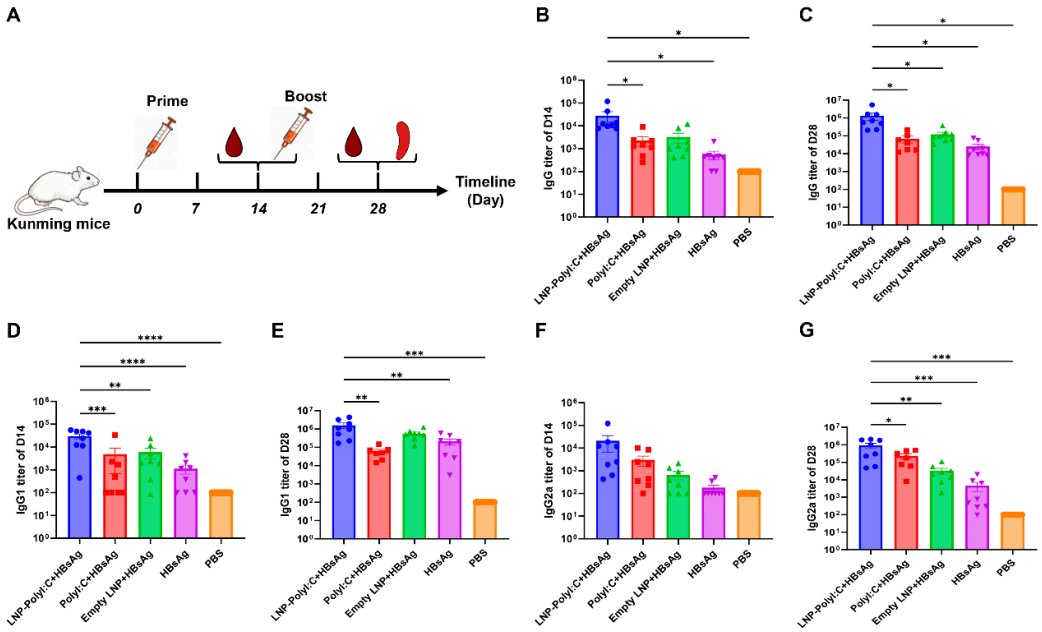


**Figure 2.** Detection of HBsAg-specific antibody expression in mouse serum by ELISA. (**A**) Schematic diagram of the mouse immunization protocol. (**B**) Levels of HBsAg-specific total IgG, (**D**) IgG1, and (**F**) IgG2a antibodies induced in serum from each treatment group on day 14 (D14) after the primary immunization. (**C**) Levels of HBsAg-specific total IgG, (**E**) IgG1, and (**G**) IgG2a antibodies induced in serum from each treatment group on day 14 (D28) after the secondary immunization. Antibody titers in all negative control groups (PBS group) were set to 100. Data represent mean ± SEM. Multiple comparisons were performed using one-way analysis of variance (ANOVA) followed by Tukey's honestly significant difference (HSD) test. $P < 0.05$ was considered statistically significant. *$P < 0.05$; **$P < 0.01$; ***$P < 0.001$; ****$P < 0.0001$.

### *3.3. The LNP-PolyI:C Adjuvant Significantly Enhances Cytokine Expression In Vivo*

Given the critical role of Th1-type and CTL-type cellular immunity in HBV prevention, the ability of the LNP-PolyI:C adjuvant to induce T-cell responses was further evaluated. The experimental procedure is shown in Figure 3A. On day 14 post-boost immunization (D28), splenocytes were isolated and stimulated with a peptide pool covering the full length of HBsAg. In flow cytometry analysis, splenocytes were stained with multiple fluorescent antibodies and analyzed using a flow cytometer. A sequential gating strategy was employed to identify the target immune cell populations (Figure 3B-F). As shown in Figures 4 and 5, the LNP-PolyI:C adjuvant group induced a robust HBsAg-specific T-cell response. The numbers of both IFN-$\gamma^+$CD4$^+$ and IFN-$\gamma^+$CD8$^+$ T cells produced in this group were significantly increased and markedly higher than those in the other four groups ($P < 0.05$). In addition to IFN-$\gamma$, CD4$^+$ T cells in the LNP-PolyI:C adjuvant group secreted a higher proportion of IL-2 and TNF-$\alpha$, while CD8$^+$ T cells secreted a higher proportion of IL-6 ($P < 0.01$). However, no significant differences in the numbers of IL-6$^+$CD4$^+$ and IL-2$^+$CD8$^+$ T cells were observed among the treatment groups ($P > 0.05$). Furthermore, the numbers of IL-4$^+$CD4$^+$, IL-4$^+$CD8$^+$, and TNF-$\alpha^+$CD8$^+$ T cells were also assessed. The results indicated that the number of IL-4$^+$CD4$^+$ T cells in the LNP-PolyI:C+HBsAg group was significantly higher than that in the PolyI:C+HBsAg and HBsAg alone groups ($P < 0.05$), but no significant difference was observed compared to the empty LNP+HBsAg and PBS groups ($P > 0.05$). The proportion of IL-4$^+$CD8$^+$ T cells in the LNP-PolyI:C+HBsAg group was comparable to that in the PolyI:C+HBsAg group ($P > 0.05$) and was significantly higher than that in the other three groups ($P < 0.05$). The number of TNF-$\alpha^+$CD8$^+$ T cells in the LNP-PolyI:C+HBsAg group was significantly higher than that in the PolyI:C+HBsAg and PBS groups ($P < 0.05$), with no significant difference compared to the empty LNP+HBsAg and HBsAg alone groups ($P > 0.05$).

 doi:10.20944/preprints202604.0040.v1



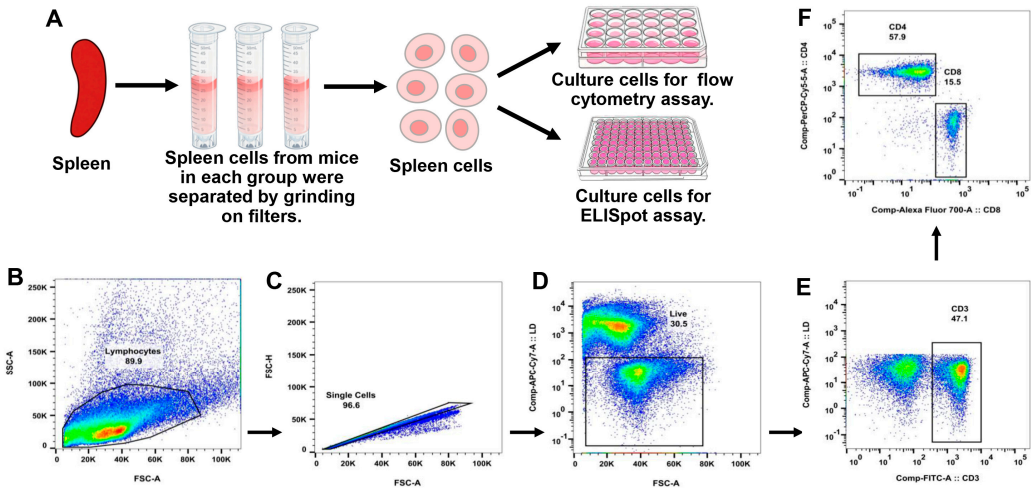


**Figure 3.** Expression profiles of various immune cells in mouse splenocytes stimulated with an HBsAg peptide library, as detected by flow cytometry. (**A**) Schematic diagram of mouse splenocyte isolation and immune stimulation. Pseudocolor plots show representative gating results close to the mean for (**B**) lymphocytes, (**C**) single cells, (**D**) live cells, (**E**) $CD3^+$ T cells, and (**F**) $CD4^+$/$CD8^+$ T cells.

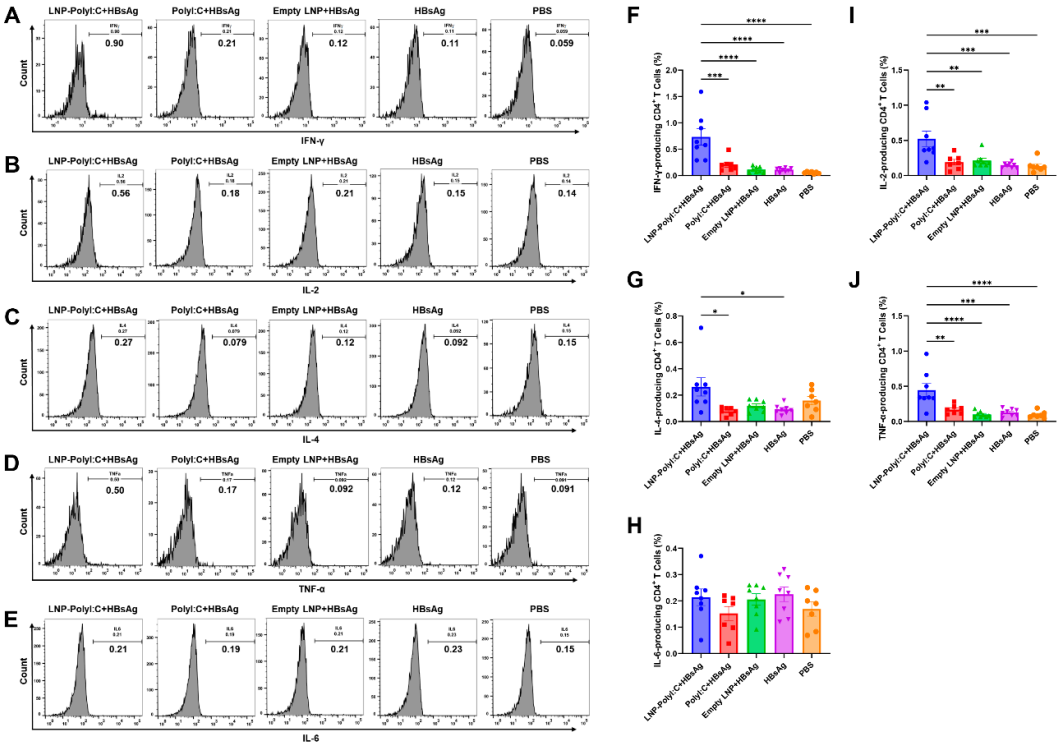


**Figure 4.** Detection of cytokine expression in $CD4^+$ T cells from mouse splenocytes stimulated with an HBsAg peptide pool by flow cytometry. Histograms show gated representative results near the mean for the expression of (**A**) IFN-γ, (**B**) IL-2, (**C**) IL-4, (**D**) TNF-α, and (**E**) IL-6. (**F-J**) Quantitative analysis of each cytokine across groups. Data represent mean ± SEM. Multiple comparisons were performed using one-way analysis of variance (ANOVA) followed by Tukey's honestly significant difference (HSD) test. $P < 0.05$ was considered statistically significant. *$P < 0.05$; **$P < 0.01$; ***$P < 0.001$; ****$P < 0.0001$.

 doi:10.20944/preprints202604.0040.v1



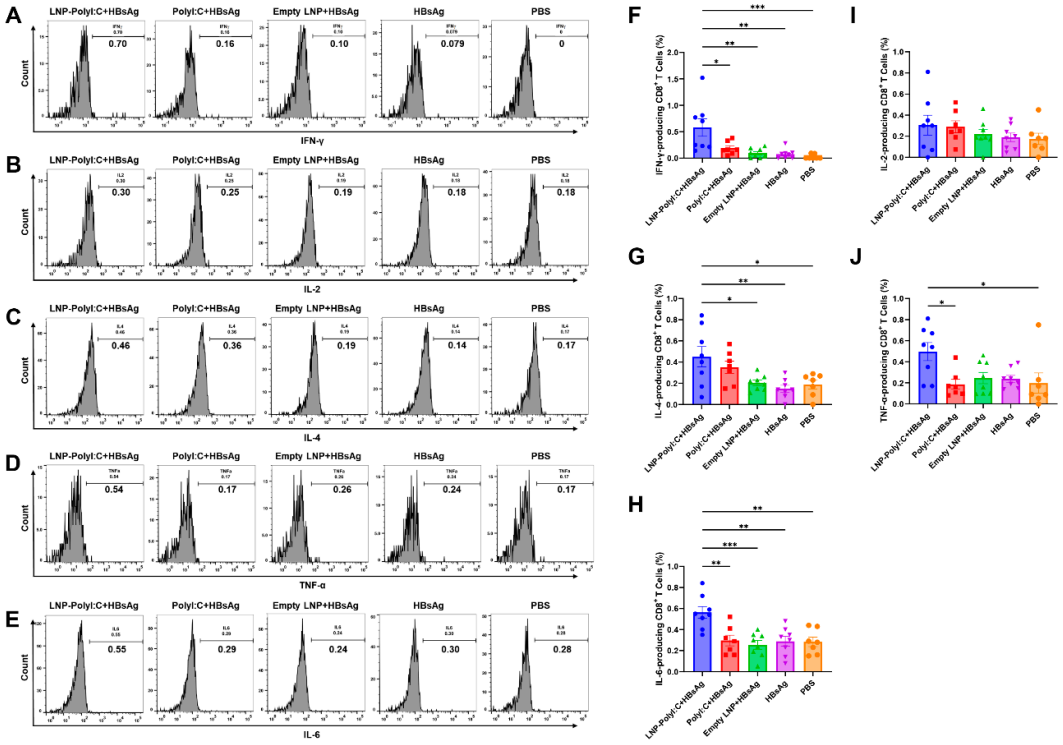


**Figure 5.** Detection of cytokine expression in CD8⁺ T cells from mouse splenocytes stimulated with an HBsAg peptide pool by flow cytometry. Histograms show gated representative results near the mean for the expression of (**A**) IFN-γ, (**B**) IL-2, (**C**) IL-4, **(**D**)** TNF-α, and (**E**) IL-6. (**F-J**) Quantitative analysis of each cytokine across groups. Data represent mean ± SEM. Multiple comparisons were performed using one-way analysis of variance (ANOVA) followed by Tukey's honestly significant difference (HSD) test. $P < 0.05$ was considered statistically significant. *$P < 0.05$; **$P < 0.01$; ***$P < 0.001$; ****$P < 0.0001$.

In addition, HBsAg-specific IFN-γ/IL-4 secreting T cells were measured by ELISpot assay in this study. As shown in Figure 6, significant differences in the magnitude of HBsAg-specific IFN-γ⁺ T-cell responses were observed among the groups. The LNP-PolyI:C+HBsAg group exhibited the highest number of SFCs per $10^6$ splenocytes (959.5 ± 127.3), followed by the PolyI:C+HBsAg group (733.3 ± 130.3). Although no statistically significant difference was observed between these two PolyI:C-containing groups ($P > 0.05$), both were significantly higher than the empty LNP+HBsAg group (76.4 ± 16.6), the HBsAg-alone group (38.4 ± 5.8), and the PBS group (30.9 ± 4.4) ($P < 0.0001$). However, no significant differences in IL-4⁺ T cell frequency were observed among the groups ($P > 0.05$). The number of SFCs per $10^6$ splenocytes for each group was as follows: LNP-PolyI:C+HBsAg group (434.8 ± 36.7), PolyI:C+HBsAg group (329.4 ± 64.6), empty LNP+HBsAg alone group (391.9 ± 57.3), HBsAg group (357.4 ± 29.8), and PBS group (352.1 ± 33.7).

 doi:10.20944/preprints202604.0040.v1



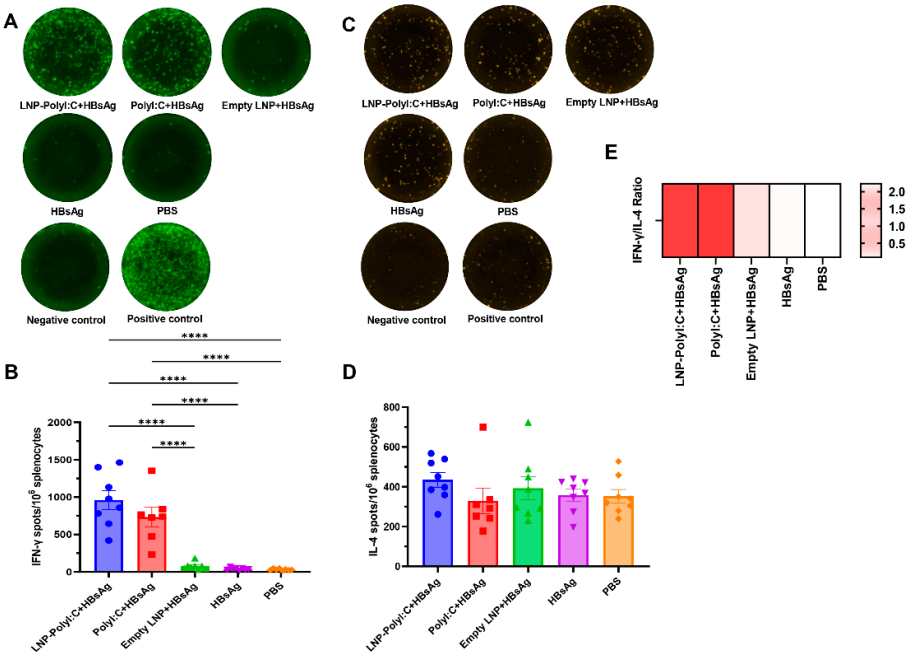


**Figure 6.** Detection of cytokine expression in mouse splenocytes stimulated with an HBsAg peptide library by Enzyme-Linked Immunospot (ELISpot). (**A**) Representative spot images of IFN-γ-secreting splenocytes and (**B**) quantitative analysis results for each group. (**C**) Representative spot images of IL-4-secreting splenocytes and (**D**) quantitative analysis results for each group. (**E**) The ratio of the average spot counts for IFN-γ to IL-4 in each group. Data represent mean ± SEM. Multiple comparisons were performed using one-way analysis of variance (ANOVA) followed by Tukey's honestly significant difference (HSD) test. $P < 0.05$ was considered statistically significant. ****$P < 0.0001$.

## 4. Discussion

Recombinant subunit antigens often require adjuvants to elicit protective immunity, yet conventional options such as alum primarily induce Th2 responses. PolyI:C, a dsRNA analog, activates both endosomal TLR3 and RLRs, thereby promoting robust Th1 and cytotoxic T lymphocyte responses, which are crucial for antiviral and anticancer vaccines. However, soluble PolyI:C suffers from nuclease degradation, poor cellular uptake, and inability to access cytoplasmic RLRs. To overcome these limitations, we propose encapsulating PolyI:C within LNPs. Leveraging mechanisms proven effective in mRNA vaccines, LNPs protect nucleic acids, enhance uptake by antigen-presenting cells, and facilitate endosomal escape. This strategy enables efficient cytoplasmic delivery of PolyI:C, thereby dual-activating TLR3 and RLRs to maximize adaptive immune responses. Against this background, this study constructed an LNP-PolyI:C adjuvant system and evaluated its potential as an adjuvant for hepatitis B vaccines.

Humoral immunity, particularly the induction of high-titer, high-affinity neutralizing antibodies, constitutes the core mechanism by which hepatitis B vaccines prevent infection. Following the entry of vaccine antigens into the body, antigen-presenting cells secrete distinct cytokines that guide the polarization of naïve $CD4^+$ T cells toward either a Th1 or Th2 phenotype[34]. Th1 cells secrete IFN-γ, which drives B cells to produce IgG2a subtype antibodies. This subtype exhibits strong complement-activating capacity and high affinity for Fc receptors, thereby effectively mediating opsonophagocytosis and the clearance of intracellular pathogens. In contrast, Th2 cells secrete IL-4, promoting B-cell class-switching toward the IgG1 subtype, which primarily exerts neutralizing activity but possesses relatively weak effector functions[35,36]. In this study, the LNP-PolyI:C adjuvant elicited high-titer, high-affinity IgG and IgG1 antibodies as early as D14. By D28, antibody titers had further increased, accompanied by a significant rise in IgG2a levels. These results

 doi:10.20944/preprints202604.0040.v1



demonstrate the advantage of the LNP-PolyI:C adjuvant in optimizing the humoral immune response of the hepatitis B vaccine. In addition, Th1 and Th2 cells form a regulatory network through the mutual antagonism of IFN-γ and IL-4, which directly determines the intensity of vaccine-induced IgG2a and IgG1 responses[37]. Therefore, the precise modulation of Th1/Th2 polarization via adjuvant selection represents a rational strategy for tailoring vaccine-induced immunity to achieve optimal protective efficacy. In this study, the IgG2a/IgG1 ratio in the LNP-PolyI:C adjuvant group remained at a relatively high level on both D14 and D28. This finding indicates that the adjuvant system effectively induced a Th2-type IgG1 response while retaining the capacity to elicit a Th1-type IgG2a response, resulting in balanced Th1/Th2 immune activation.

Previous studies have indicated that LNPs may exhibit intrinsic adjuvant activity by modulating inflammasome activation and Toll-like receptor signaling pathways to trigger inflammatory responses[38]. In the present study, we observed no significant difference in IgG1 titers between the LNP-PolyI:C group and the empty LNP group at D28. This finding indicates that the LNP carrier alone was sufficient to induce a Th2-type IgG1 response, confirming its significant intrinsic Th2 adjuvant activity. Recently, Lamoot et al.[17] similarly reported comparable levels of antigen-specific IgG1 between the empty LNP group and the LNP-PolyI:C adjuvant group in a SARS-CoV-2 vaccine study. In contrast, the primary contribution of PolyI:C was to enhance the Th1-type IgG2a response and total antibody titers, thereby promoting T cell-dependent antibody affinity maturation. The data from this study support this mechanism: following the addition of PolyI:C, IgG2a levels on both D14 and D28 showed an increasing trend, confirming the directional driving effect of TLR3 signaling on Th1 polarization.

T lymphocytes are the key effector cells of cellular immunity, comprising primarily $CD4^+$ and $CD8^+$ T cell subsets. $CD4^+$ T cells can differentiate into Th1 and Th2 subsets, which can be distinguished by the cytokines they secrete upon activation. Th1 cells produce cytokines such as IFN-γ, IL-2, and TNF-α, which promote macrophage activation and recruitment, facilitate CTL differentiation, and induce cellular immune responses. In contrast, Th2 cells produce cytokines, including IL-4 and IL-6, which promote B cell proliferation and differentiation and elicit humoral immune responses. $CD8^+$ T cells, also known as CTLs, serve as the terminal effectors of cellular immunity. They similarly secrete IFN-γ and TNF-α and directly eliminate infected target cells via the perforin/granzyme pathway or death receptor-mediated pathways[36,39]. In this study, the LNP-PolyI:C/HBsAg vaccine significantly induced HBsAg-specific Th1-type $CD4^+$ T-cell responses (IFN-$\gamma^+$, TNF-$\alpha^+$, and IL-$2^+$) and CTL-type $CD8^+$ T-cell responses (IFN-$\gamma^+$, IL-$6^+$). This indicates that the LNP-PolyI:C adjuvant system synergistically activates cellular immunity through a dual mechanism: Th1 cells amplify immune activation via classic cytokine cascades, while CTLs directly kill infected target cells. This finding is consistent with the study by Liu et al.[40] on an HBV vaccine containing LNP-PolyI:C, which also reported significant induction of IFN-$\gamma^+CD8^+$ T cells.

Notably, in the ELISpot results, the number of IFN-γ SFCs in the LNP-PolyI:C group was approximately 31% higher than that in the PolyI:C group. This suggests that LNP encapsulation facilitates intracellular delivery and endosomal escape of PolyI:C, thereby further amplifying T-cell activation via the TLR3 signaling pathway. Although the number of IFN-γ SFCs in the empty LNP adjuvant group was slightly higher than that in the antigen-alone group, it remained substantially lower than that in the PolyI:C-containing groups. This indicates that the LNP carrier itself has a limited enhancing effect on cellular immunity, whereas PolyI:C is the key determinant for inducing potent Th1/CTL responses. Furthermore, the PBS control group already exhibited a relatively high baseline level of IL-4 secretion, suggesting that this background signal may have masked the true adjuvant-induced effect on Th2 responses. Nevertheless, the IFN-γ/IL-4 ratio remained significantly higher in all PolyI:C-containing groups compared to other groups, confirming that PolyI:C induces an immune response characterized by a Th1 bias.

As a key component in enhancing the immune response, the stability of an adjuvant's physicochemical properties directly determines its immunopotentiating effect in vaccines. In this study, DLS analysis revealed that the Z-average particle size and PDI of LNP-PolyI:C increased

 doi:10.20944/preprints202604.0040.v1



initially before plateauing, suggesting that the particles may have undergone significant aggregation/fusion processes in the early stage, after which the system gradually reached a kinetically stable state. It has been reported that when lipid carriers are used for drug delivery, the PDI is typically kept below 0.3 to maintain a homogeneous population of phospholipid vesicles [41]. However, in this study, the PDI of LNP-PolyI:C exceeded 0.3 after one month of storage at 2–8 °C, indicating that further optimization of its formulation is necessary to control PDI during long-term storage. Furthermore, multiple studies have demonstrated that lyophilization can enhance the stability of mRNA-LNP vaccines[42–44]. Therefore, subsequent research will explore the application of lyophilization technology to LNP-PolyI:C/HBsAg vaccines to improve storage stability and facilitate their clinical translation.

## 5. Conclusions

In this study, a polyinosinic-polycytidylic acid adjuvant system based on lipid nanoparticles was successfully developed, and its immunogenicity and stability as a hepatitis B vaccine adjuvant were systematically evaluated. This adjuvant system significantly enhanced the immunogenicity of the hepatitis B vaccine, and the delivery efficiency of PolyI:C was significantly enhanced following LNP encapsulation. Mouse immunization experiments demonstrated that the LNP-PolyI:C adjuvant induced a potent and balanced immune response: serum levels of total IgG, IgG1, and IgG2a were significantly elevated; concomitantly, Th1-type $CD4^+$ T cell and CTL responses in the spleen were markedly enhanced. This immune profile contrasted sharply with the significant Th2 bias observed with aluminium adjuvants. In summary, the LNP-PolyI:C adjuvant holds considerable application potential for the prevention or control of viral infections, such as HBV, where synergistic cellular immunity is required for viral clearance.

**Author Contributions:** Conceptualization, Y.L. (Yuan Liu), Z.Z., H.W, and B.W.; methodology, L.Y. (Yuan Liu), and Z.Z; validation, Y.L. (Yuan Liu), Z.Z. and H.W.; formal analysis, Z.Z. and H.W.; investigation, Z.Z., Q.Z, Y.L. (Yunfei Liang); data curation, Z.Z.; writing—original draft preparation, Z.Z.; writing—review and editing, Y.L. (Yuan Liu) and H.W.; visualization, Z.Z.; supervision, Y.L. (Yuan Liu), H.W, and B.W.; project administration, Y.L. (Yuan Liu), and B.W.; funding acquisition, Y.L. (Yuan Liu), and B.W. All authors have read and agreed to the published version of the manuscript.

**Funding:** This study was sponsored by Liaoning Yisheng Biopharmaceutical Co., Ltd.

**Institutional Review Board Statement:** All animal experiments were performed at the animal facility of Liaoning Yisheng Biopharmaceutical Co., Ltd. in compliance with the Chinese guidelines for the care and use of laboratory animals. The facility and the experimental protocols were approved by the institutional review body of Liaoning Yisheng Biopharmaceutical Co., Ltd.

**Informed Consent Statement:** Not applicable.

**Data Availability Statement:** The dataset is available on request from the authors.

**Acknowledgments:** No acknowledgements apply to this work.”

**Conflicts of Interest:** The authors declare no conflicts of interest.

## Abbreviations

The following abbreviations are used in this manuscript:

| | |
|---|---|
| PolyI:C | Polyinosinic-polycytidylic acid |
| LNP | Lipid nanoparticle |
| HBsAg | Hepatitis B surface antigen |
| ELISA | Enzyme-linked immunosorbent assay |
| ELISpot | Enzyme-linked immunospot |
| CTL | Cytotoxic T lymphocyte |

 doi:10.20944/preprints202604.0040.v1



| | |
|---|---|
| HBV | Hepatitis B virus |
| APC | Antigen-presenting cell |
| TLR9 | Toll-like receptor 9 |
| dsRNA | Double-stranded RNA |
| PAMP | Pathogen-associated molecular pattern |
| MDA-5 | Melanoma differentiation–associated protein 5 |
| IRF3 | Interferon regulatory factor 3 |
| NF-κB | Nuclear factor κB |
| AP-1 | Activator protein-1 |
| CARD | Caspase recruitment domain |
| MAVS | Mitochondrial antiviral signaling |
| PBS | Phosphate-buffered saline |
| PDI | Polydispersity index |
| SPF | Specific pathogen-free |
| HRP | Horseradish peroxidase |
| BSA | Bovine serum albumin |
| TMB | Tetramethylbenzidine |
| RBC | Red blood cell |
| SFC | Spots forming cell |
| ANOVA | One-way analysis of variance |
| HSD | Honestly significant difference |
| HDF | Hydrodynamic focusing |
| DLS | Dynamic light scattering |
| DOTAP | 1,2-stearoyl-3-trimethylammonium-propane |
| DSPC | 1,2-distearoyl-sn-glycero-3-phosphocholine |
| DSPE-PEG 2000 | 1,2-distearoyl-sn-glycero-3-phosphoethanolamine-N-[methoxy(polyethylene glycol)-2000] |

## References


1. Debbag, R.; Ávila-Agüero, M.L.; Brea, J.; Espinal, C.; Romero-Feregrino, R.; Torres, J.R.; Vázquez, H.; Cuadros, R.; Lazo-Páez, G.; Schilling, A.; et al. Impact of Vaccines Across the Lifespan: A New Perspective in Public Health—Conclusions of an Expert Panel—Part 2. *Vaccines* **2026**, *14*, 204, doi:10.3390/vaccines14030204.
2. Qiu, J.; Zhang, S.; Feng, Y.; Su, X.; Cai, J.; Chen, S.; Liu, J.; Huang, S.; Huang, H.; Zhu, S.; et al. Efficacy and safety of hepatitis B vaccine: an umbrella review of meta-analyses. *Expert Rev Vaccines* **2024**, *23*, 69–81, doi:10.1080/14760584.2023.2289566.
3. Romano, L.; Paladini, S.; Galli, C.; Raimondo, G.; Pollicino, T.; Zanetti, A.R. Hepatitis B vaccination. *Hum Vaccin Immunother* **2015**, *11*, 53–57, doi:10.4161/hv.34306.
4. Reed, S.G.; Orr, M.T.; Fox, C.B. Key roles of adjuvants in modern vaccines. *Nat Med* **2013**, *19*, 1597–1608, doi:10.1038/nm.3409.
5. D'Oro, U.; O'Hagan, D.T. The scientific journey of a novel adjuvant (AS37) from bench to bedside. *NPJ Vaccines* **2024**, *9*, 26, doi:10.1038/s41541-024-00810-6.
6. Liu, X.; Min, Q.; Song, H.; Yue, A.; Li, Q.; Zhou, Q.; Han, W. Potentiating humoral and cellular immunity using a novel hybrid polymer-lipid nanoparticle adjuvant for HBsAg-VLP vaccine. *J Nanobiotechnology* **2023**, *21*, 441, doi:10.1186/s12951-023-02116-6.
7. Liao, X.; Liang, Z. Strategy vaccination against Hepatitis B in China. *Hum Vaccin Immunother* **2015**, *11*, 1534–1539, doi:10.4161/21645515.2014.980206.
8. Dolan, S.A. Vaccines for hepatitis A and B. The latest recommendations on safe and extended protection. *Postgrad Med* **1997**, *102*, 74–80, doi:10.3810/pgm.1997.12.377.
9. Sinani, G.; Senel, S. Advances in vaccine adjuvant development and future perspectives. *Drug Deliv* **2025**, *32*, 2517137, doi:10.1080/10717544.2025.2517137.
10. Hogenesch, H. Mechanism of immunopotentiation and safety of aluminum adjuvants. *Front Immunol* **2012**, *3*, 406, doi:10.3389/fimmu.2012.00406.
11. Champion, C.R. Heplisav-B: A Hepatitis B Vaccine With a Novel Adjuvant. *Ann Pharmacother* **2021**, *55*, 783–791, doi:10.1177/1060028020962050.

 doi:10.20944/preprints202604.0040.v1




12. Alexopoulou, L.; Holt, A.C.; Medzhitov, R.; Flavell, R.A. Recognition of double-stranded RNA and activation of NF-kappaB by Toll-like receptor 3. *Nature* **2001**, *413*, 732–738, doi:10.1038/35099560.
13. Rehwinkel, J.; Gack, M.U. RIG-I-like receptors: their regulation and roles in RNA sensing. *Nat Rev Immunol* **2020**, *20*, 537–551, doi:10.1038/s41577-020-0288-3.
14. Chin, A.I.; Miyahira, A.K.; Covarrubias, A.; Teague, J.; Guo, B.; Dempsey, P.W.; Cheng, G. Toll-like receptor 3-mediated suppression of TRAMP prostate cancer shows the critical role of type I interferons in tumor immune surveillance. *Cancer Res* **2010**, *70*, 2595–2603, doi:10.1158/0008-5472.CAN-09-1162.
15. Akazawa, T.; Ebihara, T.; Okuno, M.; Okuda, Y.; Shingai, M.; Tsujimura, K.; Takahashi, T.; Ikawa, M.; Okabe, M.; Inoue, N.; et al. Antitumor NK activation induced by the Toll-like receptor 3-TICAM-1 (TRIF) pathway in myeloid dendritic cells. *Proc Natl Acad Sci U S A* **2007**, *104*, 252–257, doi:10.1073/pnas.0605978104.
16. Cheng, Y.S.; Xu, F. Anticancer function of polyinosinic-polycytidylic acid. *Cancer Biol Ther* **2010**, *10*, 1219–1223, doi:10.4161/cbt.10.12.13450.
17. Lamoot, A.; Jangra, S.; Laghlali, G.; Warang, P.; Singh, G.; Chang, L.A.; Park, S.C.; Singh, G.; De Swarte, K.; Zhong, Z.; et al. Lipid Nanoparticle Encapsulation Empowers Poly(I:C) to Activate Cytoplasmic RLRs and Thereby Increases Its Adjuvanticity. *Small* **2024**, *20*, e2306892, doi:10.1002/smll.202306892.
18. Lang, K.S.; Recher, M.; Junt, T.; Navarini, A.A.; Harris, N.L.; Freigang, S.; Odermatt, B.; Conrad, C.; Ittner, L.M.; Bauer, S.; et al. Toll-like receptor engagement converts T-cell autoreactivity into overt autoimmune disease. *Nat Med* **2005**, *11*, 138–145, doi:10.1038/nm1176.
19. Walters, A.A.; Qin, Y.; Saleh, A.F.; Cheung, C.C.L.; Lyu, Q.; Zhu, Z.; Gafar, H.A.M.; Tzu-Wen Wang, J.; Al-Jamal, K.T. Triplet RNA Lipid Nanoparticles for Locoregional Cancer Immunotherapy. *Small Sci* **2026**, *6*, e202500506, doi:10.1002/smsc.202500506.
20. DeMuth, P.C.; Min, Y.; Huang, B.; Kramer, J.A.; Miller, A.D.; Barouch, D.H.; Hammond, P.T.; Irvine, D.J. Polymer multilayer tattooing for enhanced DNA vaccination. *Nat Mater* **2013**, *12*, 367–376, doi:10.1038/nmat3550.
21. Rwandamuriye, F.X.; Evans, C.W.; Wylie, B.; Norret, M.; Vitali, B.; Ho, D.; Nguyen, D.; Roper, E.A.; Wang, T.; Hepburn, M.S.; et al. A surgically optimized intraoperative poly(I:C)-releasing hydrogel prevents cancer recurrence. *Cell Rep Med* **2023**, *4*, 101113, doi:10.1016/j.xcrm.2023.101113.
22. Song, H.; Huang, P.; Niu, J.; Shi, G.; Zhang, C.; Kong, D.; Wang, W. Injectable polypeptide hydrogel for dual-delivery of antigen and TLR3 agonist to modulate dendritic cells in vivo and enhance potent cytotoxic T-lymphocyte response against melanoma. *Biomaterials* **2018**, *159*, 119–129, doi:10.1016/j.biomaterials.2018.01.004.
23. Jewell, C.M.; Lopez, S.C.; Irvine, D.J. In situ engineering of the lymph node microenvironment via intranodal injection of adjuvant-releasing polymer particles. *Proc Natl Acad Sci U S A* **2011**, *108*, 15745–15750, doi:10.1073/pnas.1105200108.
24. Koerner, J.; Horvath, D.; Herrmann, V.L.; MacKerracher, A.; Gander, B.; Yagita, H.; Rohayem, J.; Groettrup, M. PLGA-particle vaccine carrying TLR3/RIG-I ligand Riboxxim synergizes with immune checkpoint blockade for effective anti-cancer immunotherapy. *Nat Commun* **2021**, *12*, 2935, doi:10.1038/s41467-021-23244-3.
25. Ko, K.H.; Lee, S.H.; Choi, Y.H.; Kang, S.M.; Yang, H.S.; Lee, S.M.; Jo, E.B.; Bae, H.S.; Hong, S.B.; Kim, D.H.; et al. Lipid nanoparticle encapsulated TLR3 agonist adjuvant elicits potent T cell immunity against cancer and viruses. *NPJ Vaccines* **2025**, *11*, 26, doi:10.1038/s41541-025-01349-w.
26. Luo, Y.; Li, Q.; Zhou, S.; Oh, H.; Jablonski, J.; Song, Y.; Su, Y.; Wu, Y.; Zhu, H.; Ortega, J.; et al. Lipid nanoparticles that co-deliver poly(I:C) and short peptide antigens elicit anti-tumor responses with vaccination. *Biomaterials* **2026**, *327*, 123754, doi:10.1016/j.biomaterials.2025.123754.
27. Polack, F.P.; Thomas, S.J.; Kitchin, N.; Absalon, J.; Gurtman, A.; Lockhart, S.; Perez, J.L.; Perez Marc, G.; Moreira, E.D.; Zerbini, C.; et al. Safety and Efficacy of the BNT162b2 mRNA Covid-19 Vaccine. *N Engl J Med* **2020**, *383*, 2603–2615, doi:10.1056/NEJMoa2034577.
28. Baden, L.R.; El Sahly, H.M.; Essink, B.; Kotloff, K.; Frey, S.; Novak, R.; Diemert, D.; Spector, S.A.; Rouphael, N.; Creech, C.B.; et al. Efficacy and Safety of the mRNA-1273 SARS-CoV-2 Vaccine. *N Engl J Med* **2021**, *384*, 403–416, doi:10.1056/NEJMoa2035389.

 doi:10.20944/preprints202604.0040.v1




29. Hald Albertsen, C.; Kulkarni, J.A.; Witzigmann, D.; Lind, M.; Petersson, K.; Simonsen, J.B. The role of lipid components in lipid nanoparticles for vaccines and gene therapy. *Adv Drug Deliv Rev* **2022**, *188*, 114416, doi:10.1016/j.addr.2022.114416.
30. Chen, S.P.; Blakney, A.K. Immune response to the components of lipid nanoparticles for ribonucleic acid therapeutics. *Curr Opin Biotechnol* **2024**, *85*, 103049, doi:10.1016/j.copbio.2023.103049.
31. Hou, X.; Zaks, T.; Langer, R.; Dong, Y. Lipid nanoparticles for mRNA delivery. *Nat Rev Mater* **2021**, *6*, 1078–1094, doi:10.1038/s41578-021-00358-0.
32. Aldosari, B.N.; Alfagih, I.M.; Almurshedi, A.S. Lipid Nanoparticles as Delivery Systems for RNA-Based Vaccines. *Pharmaceutics* **2021**, *13*, doi:10.3390/pharmaceutics13020206.
33. Singh, V.; Chernatynskaya, A.; Qi, L.; Chuang, H.Y.; Cole, T.; Jeyalatha, V.M.; Bhargava, L.; Yeudall, W.A.; Farkas, L.; Yang, H. Liposomes-Encapsulating Double-Stranded Nucleic Acid (Poly I:C) for Head and Neck Cancer Treatment. *ACS Pharmacol Transl Sci* **2024**, *7*, 1612–1623, doi:10.1021/acsptsci.4c00121.
34. Ruterbusch, M.; Pruner, K.B.; Shehata, L.; Pepper, M. In Vivo CD4(+) T Cell Differentiation and Function: Revisiting the Th1/Th2 Paradigm. *Annu Rev Immunol* **2020**, *38*, 705–725, doi:10.1146/annurev-immunol-103019-085803.
35. Chin'ombe, N.; Bourn, W.R.; Williamson, A.-L.; Shephard, E.G. Oral vaccination with a recombinant Salmonella vaccine vector provokes systemic HIV-1 subtype C Gag-specific CD4+ Th1 and Th2 cell immune responses in mice. *Virology Journal* **2009**, *6*, 87, doi:10.1186/1743-422X-6-87.
36. Chung, N.H.; Chen, Y.C.; Yang, S.J.; Lin, Y.C.; Dou, H.Y.; Hui-Ching Wang, L.; Liao, C.L.; Chow, Y.H. Induction of Th1 and Th2 in the protection against SARS-CoV-2 through mucosal delivery of an adenovirus vaccine expressing an engineered spike protein. *Vaccine* **2022**, *40*, 574–586, doi:10.1016/j.vaccine.2021.12.024.
37. Paludan, S.R. Interleukin-4 and interferon-gamma: the quintessence of a mutual antagonistic relationship. *Scand J Immunol* **1998**, *48*, 459–468, doi:10.1046/j.1365-3083.1998.00435.x.
38. Kedmi, R.; Ben-Arie, N.; Peer, D. The systemic toxicity of positively charged lipid nanoparticles and the role of Toll-like receptor 4 in immune activation. *Biomaterials* **2010**, *31*, 6867–6875, doi:10.1016/j.biomaterials.2010.05.027.
39. Gao, S.; Yang, D.; Fang, Y.; Lin, X.; Jin, X.; Wang, Q.; Wang, X.; Ke, L.; Shi, K. Engineering Nanoparticles for Targeted Remodeling of the Tumor Microenvironment to Improve Cancer Immunotherapy. *Theranostics* **2019**, *9*, 126–151, doi:10.7150/thno.29431.
40. Liu, X.; Min, Q.; Li, Y.; Chen, S. Enhanced Cellular Immunity for Hepatitis B Virus Vaccine: A Novel Polyinosinic-Polycytidylic Acid-Incorporated Adjuvant Leveraging Cytoplasmic Retinoic Acid-Inducible Gene-Like Receptor Activation and Increased Antigen Uptake. *Biomaterials Research* **2024**, *28*, 0096, doi:doi:10.34133/bmr.0096.
41. Danaei, M.; Dehghankhold, M.; Ataei, S.; Hasanzadeh Davarani, F.; Javanmard, R.; Dokhani, A.; Khorasani, S.; Mozafari, M.R. Impact of Particle Size and Polydispersity Index on the Clinical Applications of Lipidic Nanocarrier Systems. *Pharmaceutics* **2018**, *10*, 57, doi:10.3390/pharmaceutics10020057.
42. Muramatsu, H.; Lam, K.; Bajusz, C.; Laczko, D.; Kariko, K.; Schreiner, P.; Martin, A.; Lutwyche, P.; Heyes, J.; Pardi, N. Lyophilization provides long-term stability for a lipid nanoparticle-formulated, nucleoside-modified mRNA vaccine. *Mol Ther* **2022**, *30*, 1941–1951, doi:10.1016/j.ymthe.2022.02.001.
43. Alejo, T.; Toro-Córdova, A.; Fernández, L.; Rivero, A.; Stoian, A.M.; Pérez, L.; Navarro, V.; Martínez-Oliván, J.; de Miguel, D. Comprehensive Optimization of a Freeze-Drying Process Achieving Enhanced Long-Term Stability and In Vivo Performance of Lyophilized mRNA-LNPs. *Int J Mol Sci* **2024**, *25*, 10603, doi:10.3390/ijms251910603.
44. Khan, M.F.H.; Sudalaiyadum Perumal, A.; Kamen, A.A. Investigation on a Freeze-Drying Process for Long-Term Stability of mRNA-LNPs. *Vaccines* **2026**, *14*, 242, doi:10.3390/vaccines14030242.